Sustainable Cities and Society 133 (2025) 106843

Contents lists available at ScienceDirect

Sustainable Cities and Society

journal homepage: www.elsevier.com/locate/scs

Harnessing green infrastructure for urban heat island mitigation: Evidence-based strategies for sustainable and climate-resilient cities

Yujing Bai [a], Yangang Xing [b,*]

[a] School of Architecture, Tianjin Chengjian University, 26 Jinjing Road, Xiqing District, Tianjin 300384, China
[b] School of Architecture, Design and the Built Environment, Nottingham Trent University, 50 Shakespeare Street, Nottingham NG1 4FQ, UK

ARTICLE INFO

Keywords:
SUHII
Vegetation fraction
Landsat
CFD
Nature-based solutions
Sustainable cities
Climate-resilient cities

ABSTRACT

The urban heat island (UHI) effect poses a significant environmental and public health challenge, particularly in the context of climate change. While urban green infrastructure (UGI) is widely recognised for its cooling potential, its implementation and effectiveness in complex, high-density urban environments, especially in extremely cold climate cities, require a comprehensive multi-scale assessment. This study presents a holistic framework that integrates seasonal variability, socioeconomic transitions, and spatial heterogeneity to evaluate UHI mitigation strategies. Drawing on satellite imagery (Landsat and MODIS), land use surveys, socioeconomic regression analysis, and computational fluid dynamics (CFD) simulations using ENVI-MET 4.0, the study identifies UHI hotspots and assesses incremental, space-efficient greening interventions. A longitudinal case study (2000–2020) in a severely cold climate city in northeast China reveals that population decline did not reverse UHI or UGI trends, as the extent of built-up areas remained largely unchanged. The findings demonstrate that green roofs provide significant cooling benefits in high-density urban settings while also enhancing thermal regulation during winter months. By integrating analyses across multiple scales, this research offers a robust methodology for quantifying UHI mitigation potential and informing data-driven urban greening strategies. The study refines vegetation metrics using land survey data, challenges assumptions about seasonal UHI dynamics, and highlights the urgent need for targeted green infrastructure in both growing and shrinking urban contexts. Overall, the research contributes to a deeper understanding of green retrofitting in extreme climates and identifies future directions for policy development, design optimisation, and interdisciplinary approaches to climate-resilient urban planning.

1. Introduction

The Urban Heat Island (UHI) phenomenon has become an increasingly critical environmental and public health challenge worldwide. UHI refers to the temperature difference between urban areas and their surrounding rural counterparts, primarily driven by anthropogenic heat emissions, impervious surfaces, and reduced vegetation cover. The intensity of Surface Urban Heat Island (SUHII) varies significantly due to factors such as urban morphology, land use patterns, population density, seasonal variations, and climate zones (Du et al., 2021; L. Li & Zha, 2019; Tran et al., 2006; J. X. Yang et al., 2021). Research indicates that UHI can contribute to biodiversity loss (Reid, 1998), degradation of air and water quality (Grimm et al., 2008), climate alterations (Hales, 2016; Jin et al., 2005), and increased morbidity and mortality rates (Luber & McGeehin, 2008; Tan et al., 2010). Additionally, UHI has been linked to shortened life expectancy (Patz et al., 2005), higher risks of violence (Gong et al., 2012), and mental health issues such as depression (Sundquist et al., 2004). Addressing UHI is therefore crucial for promoting sustainable urban development and enhancing public well-being (Xing, 2024a,b, 2025).

A key driver of UHI is rapid urbanisation, which induces Land Use/Land Cover (LULC) transformations, resulting in the loss of natural landscapes and increased surface heat retention (Amiri et al., 2009; Chen et al., 2006; Hu & Jia, 2010; Jusuf et al., 2007; Kawamoto, 2016; Singh et al., 2017). Consequently, urban green infrastructure (UGI) has emerged as a promising nature-based solution to mitigate UHI effects (Lehmann, 2014; Y. Li et al., 2023; QIU et al., 2013). UGI refers to interconnected networks of vegetative and water-based ecosystems, including parks, forests, grasslands, urban agriculture, green roofs, and water bodies (Ely & Pitman, 2014; Naumann et al., 2011; The North

* Corresponding author: School of Architecture, Design and the Built Environment, Nottingham Trent University, 50 Shakespeare Street, Nottingham NG1 4FQ, UK.
E-mail addresses: hitashley1214@outlook.com (Y. Bai), yangang.xing@ntu.ac.uk (Y. Xing).

https://doi.org/10.1016/j.scs.2025.106843
Received 19 April 2025; Received in revised form 19 September 2025; Accepted 19 September 2025
Available online 20 September 2025
2210-6707/© 2025 The Authors. Published by Elsevier Ltd. This is an open access article under the CC BY license (http://creativecommons.org/licenses/by/4.0/).

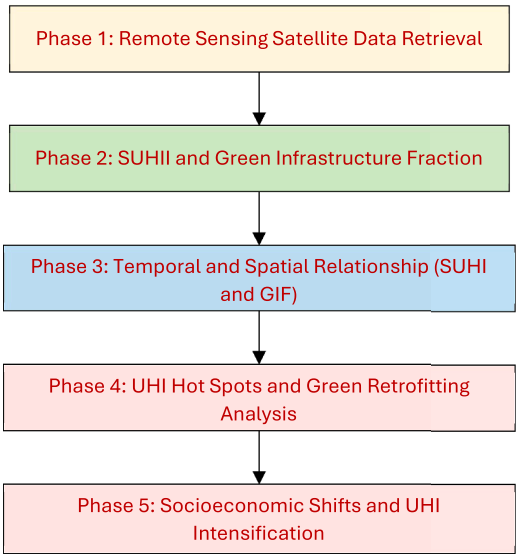

Fig. 1. A Generic Holistic Analytic Framework to Support Urban Retrofitting Decision Making.

West Green Infrastructure Think Tank, 2008). Several studies have demonstrated that increased vegetation cover is inversely correlated with land surface temperature (LST) in diverse climate zones (Bai et al., 2018; Greene & Kedron, 2018; Jenerette et al., 2007; X. Li et al., 2013; Ma et al., 2008; Y. Wang & Akbari, 2016a; T. Wang et al., 2022; Weng et al., 2004; Zhou et al., 2011).

A number of studied explored correlation coefficients between green vegetation fraction and land surface temperature (LST) across various Köppen climate classifications. Most studies found a significant negative correlation, indicating that increased vegetation cover generally reduces LST. For instance, Li, Zhang and Kainz (2012) reported a strong negative correlation ($R = -0.81$) in a CFa climate, while Weng, Rajasekar and Hu (2011) found even stronger correlations ($R = -0.98$) in a DFa climate. The significance levels (P) in these studies were mostly below 0.01, confirming the reliability of the correlations. However, some studies, such as Wang and Akbari (2016b), observed positive correlations during specific times of the day, highlighting the complexity of the relationship between vegetation cover and LST. Overall, the findings in the existing literature underscore the importance of green infrastructure in mitigating urban heat island effects across different climates and land use types. Furthermore, different types of green infrastructure exhibit varying cooling potentials. Empirical studies suggest that urban parks can reduce LST by 0.1 °C to 6.7 °C, with cooling effects extending about 1000 m beyond park boundaries. The extent of cooling depends on park size, species composition, and spatial configuration (Feyisa et al., 2014; T. Wang et al., 2022). Similarly, water bodies exert significant cooling effects through evapotranspiration, lowering ambient temperatures by 1 °C to 4 °C (Sun et al., 2012). Urban agriculture has also been shown to reduce local temperatures by 0.5 °C to 4 °C (QIU et al., 2013). In high-density urban areas, green roof infrastructure can lower ambient temperatures by 1 °C to 2 °C, provided there is sufficient moisture availability (Bass et al., 2002).

Despite increasing research on the urban heat island (UHI) effect, several critical gaps remain. Most existing studies focus on temperate or hot climates, with limited attention to cold-climate cities where seasonal thermal dynamics and vegetation responses differ significantly (García-Cueto et al., 2007; He et al., 2007; Yang et al., 2020). This limits the applicability of current UHI mitigation strategies across diverse climatic contexts. Moreover, while rapid urbanisation is widely recognised as a major driver of UHI (Mathew et al., 2017; Singh et al., 2017), the thermal implications of urban depopulation remain underexplored. Population decline does not necessarily result in reduced UHI intensity, particularly when it is accompanied by continued urban expansion and a lack of investment in green infrastructure. In addition, existing UHI mitigation strategies have primarily targeted growing cities, overlooking the emerging risks faced by shrinking cities. There is a pressing need for integrated, context-sensitive approaches that account for socioeconomic transitions, seasonal variability, and spatial heterogeneity. Furthermore, few studies employ a multi-scale analytical framework capable of linking meso-scale (e.g. 1.2 km grids) assessments with micro-scale, building-level simulations. Such integration is essential for designing spatially adaptive and thermally effective interventions. This study addresses these gaps by applying a multi-level, seasonally informed framework to analyse UHI dynamics and evaluate green infrastructure solutions in an extremely cold-climate urban context.

2. Methodology

A holistic methodological framework (Fig. 1) is created in this paper for assisting urban green retrofitting decision-making, integrating multi-source data and computational modelling techniques. The framework begins with the collection of socio-economic data, remote sensing data, and land use/land cover (LULC) data, which serve as key inputs for analysing urban heat island (UHI) dynamics. From remote sensing data, land surface temperature (LST) and Surface Urban Heat Island Intensity (SUHII) are retrieved, while LULC data contribute to the calculation of the green infrastructure fraction. These datasets are then processed through linear regression analysis, establishing relationships between UHI intensity and green infrastructure distribution. Identified UHI hotspots inform the next stage, where Computational Fluid Dynamics (CFD) simulations are employed to model different urban green retrofitting scenarios. The results from CFD simulations support evidence-based decision-making for urban green infrastructure planning, facilitating the development of effective UHI mitigation strategies tailored to complex urban environments.

2.1. Phase 1: land surface temperature (LST) retrieval and accuracy enhancement

This study employs the radiative transfer equation (RTE) method for land surface temperature (LST) retrieval, as it has been demonstrated to provide superior accuracy compared to alternative methods such as the mono-window, single-channel, and split-window algorithms (José A. Sobrino et al., 2004; Yu et al., 2014). Existing LST retrieval approaches include the RTE method (Yu et al., 2014), mono-window algorithm (Singh et al., 2017; Zandi et al., 2022), single-channel method (Jiménez-Muñoz, 2003; Walawender et al., 2014), split-window algorithm(J. A. Sobrino & Raissouni, 2000; Wan, 1996), multi-channel and multi-angle algorithms (J. A. Sobrino et al., 1996), and emissivity-corrected methods (Son et al., 2017; C. Yang et al., 2020). Comparative analyses indicate that the RTE method consistently yields the most accurate results, with biases for Landsat 8 data of 0.06 K (band 10) using RTE, 0.44 K using the single-channel method, and −0.15 K using the split-window algorithm (Yu et al., 2014). Similarly, for Landsat 5 data, the biases are −0.17 K for the RTE method, 2.09 K for the mono-window algorithm, and 0.78 K for the single-channel method (José A. Sobrino et al., 2004). Kan, Liu and Li (2016) further confirm that the RTE method provides LST estimations closest to ground measurements compared to the single-channel and split-window approaches. This study enhances LST retrieval accuracy by incorporating spatio-temporal corrections and emissivity calibration, ensuring more robust estimations from Landsat 5, 7, and 8 datasets. By refining temperature retrievals, this methodology strengthens the reliability of surface urban heat island intensity (SUHII) analysis. In accordance with the RTE framework, the thermal infrared radiance value (L_λ) is consist of the atmospheric upwelling radiance ($L_\uparrow$), the atmospheric downwelling radiance ($L_\downarrow$), and the land surface radiance. It can be expressed in Eq. (1) (José A. Sobrino et al., 2004; Yu et al., 2014):

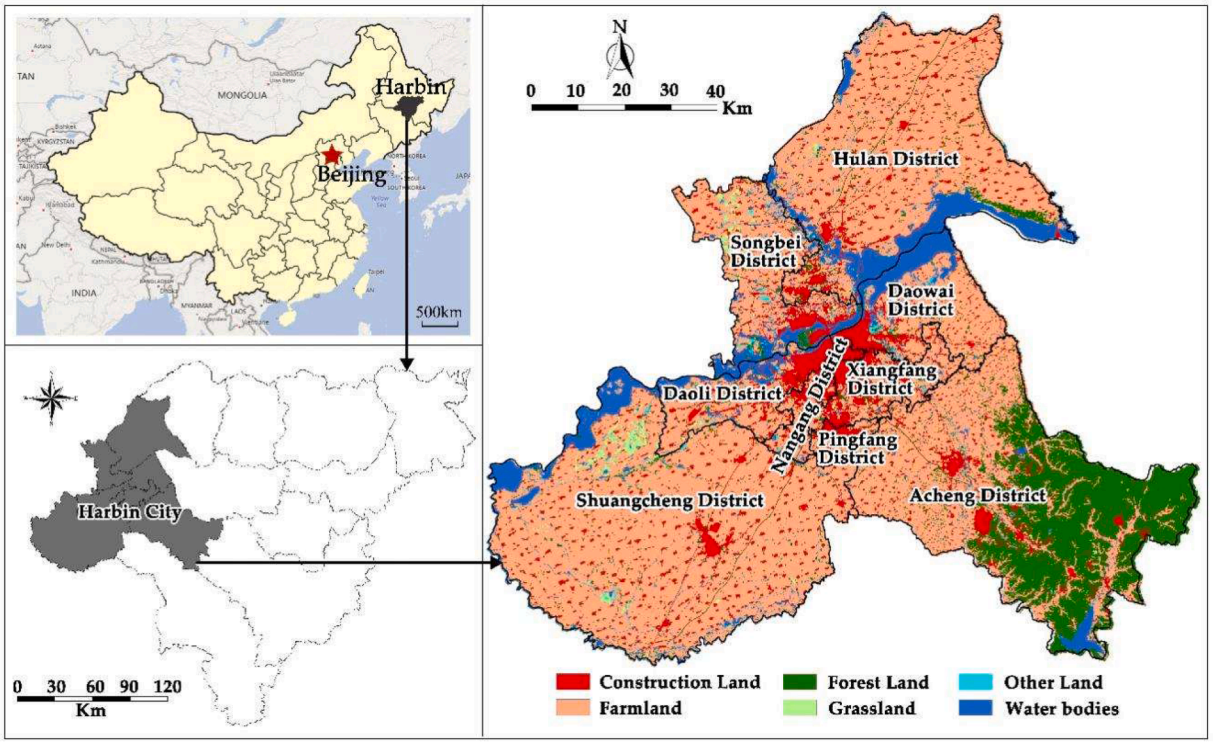

Fig. 2. Geographical location of study area - Harbin (45°08'~46°25'N, 125°41'~127°39'E).

$$L_\lambda = [\varepsilon B(T_s) + (1-\varepsilon)L_\downarrow]\tau + L_\uparrow, \quad (1)$$

Where T_s is the real LST; $B(T_s)$ is the thermal radiance of a blackbody (the earth's surface) when the temperature is T_s; τ is the atmospheric transmissivity in the thermal infrared band; ε is the land surface emissivity which can calculate according to Qin et al. (2004). The parameters $L_\uparrow$, $L_\downarrow$, τ can obtain through a web-based atmospheric correction parameter calculator (J. A. Barsi et al., 2003; Julia A Barsi et al., 2005). Thus, the equation of the blackbody radiance ($B(Ts)$) can be deduced (José A. Sobrino et al., 2004):

$$B(T_s) = [L_\lambda - L_\uparrow - \tau(1-\varepsilon) \times L_\downarrow]/(\tau\varepsilon), \quad (2)$$

At last, T_s can be obtained using the inversion of the Planck's law (Eq. (3)) (José A. Sobrino et al., 2004),

$$T_s = \frac{K_2}{\ln(K_1/B(T_s)+1)}, \quad (3)$$

For the Landsat 5 TM, $K_1 = 607.76$ W/(m^2·sr·μm), $K_2 = 1260.56$ K. For the Landsat 7 ETM+, $K_1 = 666.09$ W/(m^2·sr·μm), $K_2 = 1282.71$ K. For the band 10 of the Landsat 8 TIRS, $K_1 = 774.89$ W/(m^2·sr·μm), $K_2 = 1321.08$ K. The results can be expressed in degrees centigrade by subtracting 273.15 from their value in Kelvin.

In the meanwhile, to improve the spatiotemporal continuity and robustness of the analysis, this study also uses MODIS data to obtain daytime and nighttime LST. The calculated equation is shown as followed:

$$T_s(^\circ\mathrm{C}) = B_1 \times S_f + A_O - 273.15, \quad (4)$$

Where B_1 is the scientific data sets named LST; S_f is the scale factor of scientific data set, here it is 0.02; A_O is additive offset of scientific data set, here it is 0.

Finally, obtained LST from MODIS and Landsat data is incorporated by gap-filling algorithms to improve the spatiotemporal continuity.

2.2. Phase 2: surface UHI intensity (SUHII) determination and green infrastructure fraction calculations

The surface UHI in this study refers to the phenomenon that the temperature of urban areas is higher than that of the surrounding rural areas (Maimaitiyiming et al., 2014; Oke, 1973). Therefore, the SUHII can determine by the mean LST difference between urban areas and suburbs. According to the mean LST distribution in Harbin city, the Acheng District, the Hulan District, and the Shuangcheng District are selected as the suburbs. To investigate the relationship between the SUHI and the green infrastructure fraction, the study calculates the SUHII in the subarea scale and 1200 m x 1200 m grid-scale, respectively.

The Normalized Difference Vegetation Index (NDVI) is often used as an indicator of green infrastructure coverage. However, NDVI has several limitations. For example, during early crop growth stages, when green leaf area is small, NDVI is highly sensitive to soil background effects (EARTH OBSERVING SYSTEM, 2019). Additionally, NDVI may saturate at later growth stages when crops reach canopy closure, leading to inaccurate results (EARTH OBSERVING SYSTEM, 2019). Furthermore, the presence of clouds and snow can interfere with NDVI values, as water bodies are indistinguishable from snow and clouds when NDVI values fall below zero (Saravanan et al., 2018).

To address these limitations, this study replaces NDVI with a green infrastructure fraction index to investigate the relationship between land use and land cover (LULC) changes and surface urban heat island (SUHI) effects (Ma et al., 2008; Weng et al., 2004). By developing linear regression models incorporating NDVI and SUHII, this study evaluates whether using the green infrastructure fraction provides an advantage over NDVI in this context.

Land use types are reclassified according to the Ministry of Land and Resources of the People's Republic of China (2013) into farmland, forest land, grassland, construction land, water bodies, and other land Zhang and Xia., 2024. Among these, farmland, forest land, grassland, and water bodies are considered green infrastructure. The green infrastructure fraction (GIF) is then calculated as the proportion of green infrastructure area relative to total land area. At the subarea scale, GIF is calculated for

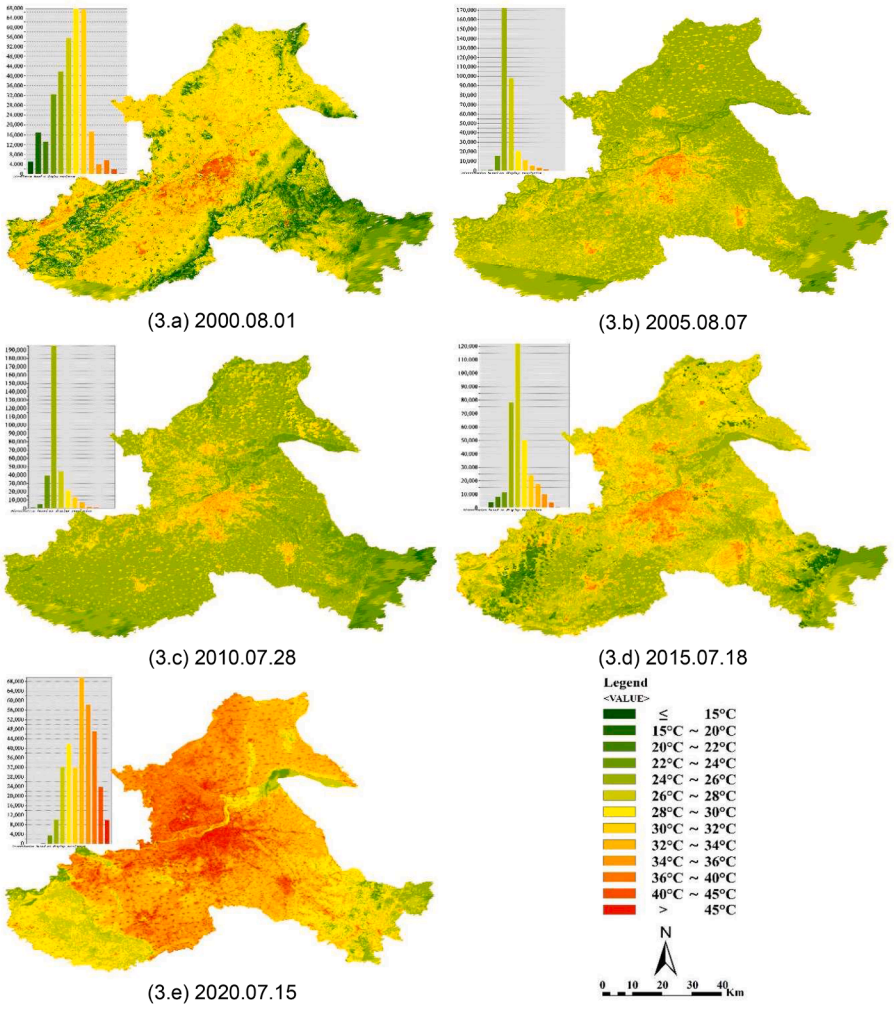

Fig. 3. The LST patterns and distribution histograms of Harbin city in the summer day (2000–2020).

each district, whereas for the grid-scale analysis, it is computed based on grid units.

2.3. Phase 3: analysis of the relationship between SUHI and green infrastructure

Fractional vegetation cover is commonly used as an indicator of vegetation abundance to examine the correlation between LULC and LST/SUHII (Amiri et al., 2009; Weng et al., 2004; Zhou et al., 2011). One widely used approach to assess the relationship between vegetation cover and SUHI is statistical analysis, including correlation and regression analyses (Cui & Foy, 2012; Greene & Kedron, 2018; Jenerette et al., 2007; X. Li et al., 2013; Y. Y. Li et al., 2012; Ma et al., 2008; Y. Wang & Akbari, 2016a; Weng et al., 2004, 2011; Zhou et al., 2011).

This study employs linear regression analysis to assess the relationship between green infrastructure and SUHI. Several simple linear regression models are developed, treating the green infrastructure fraction as the independent variable and SUHII as the dependent variable. Additionally, models incorporating NDVI and SUHII are built to compare the effectiveness of using the green infrastructure fraction instead of NDVI in this context.

2.4. Phase 4: urban green retrofitting decision making and detailed case study

To further investigate the influence of green infrastructure on UHI, the study uses the ENVI-MET software to simulate air temperature changes under different green infrastructure fraction scenarios. Based on the spatial distribution of LST and SUHII, urban heat hotspots are identified. One of these hotspots is selected for the development of multi-scenario 3D models, each representing a different green retrofitting strategy. Comparing the effectiveness of different strategies in mitigating UHI provides insights for future land use planning and decision-making.

2.5. Phase 5: socioeconomic shifts and UHI intensification

In this phase, we explored the relationship between surface urban heat island intensity (SUHII) and key socioeconomic indicators, including population density, gross domestic product (GDP), and the green infrastructure fraction (GIF). SUHII data were extracted from remote sensing imagery, while socioeconomic and land use information was sourced from statistical yearbooks and LULC datasets. The aim was to identify patterns and associations between socioeconomic dynamics and urban thermal behaviour. Particular attention was given to how population decline, economic shifts, and variations in green infrastructure relate to changes in SUHII, especially in the context of an extremely cold-climate city.

2.6. A case study

A detailed case study of Harbin is developed based on this framework

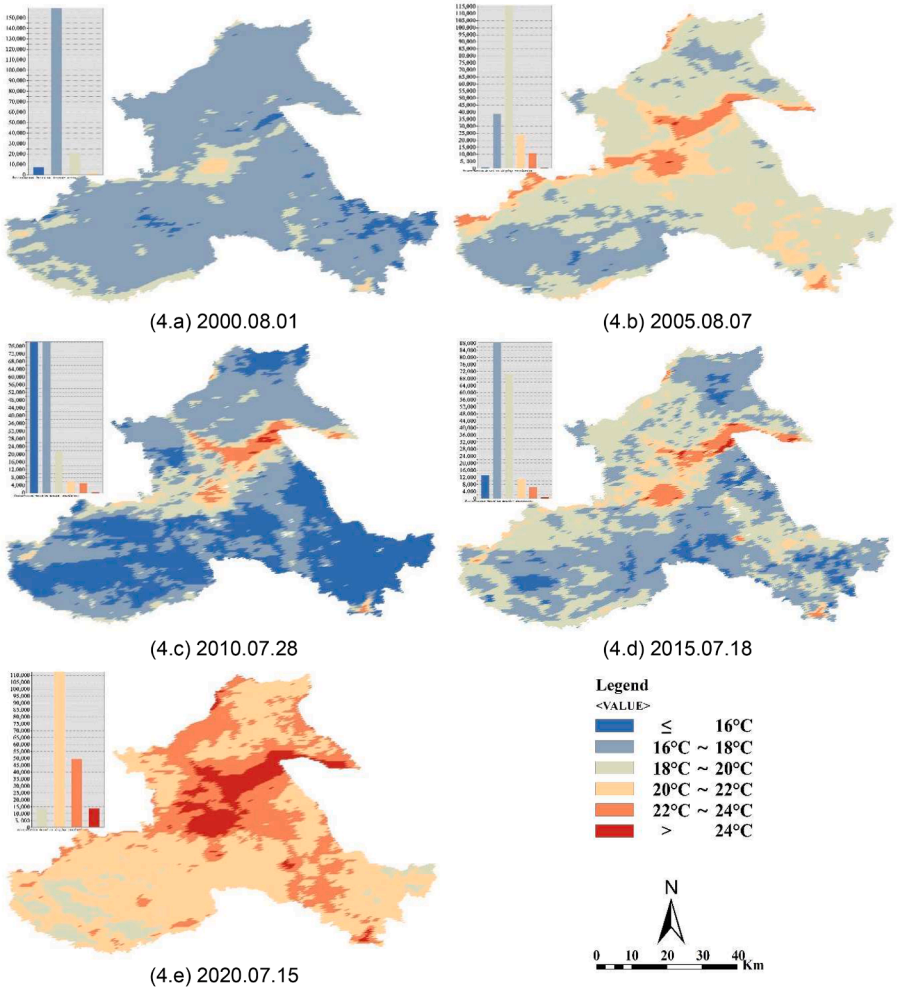

Fig. 4. The LST patterns and distribution histograms of Harbin city in the summer night (2000–2020).

(Fig. 1). Harbin (DWa climate zone) located in northeastern China, is the capital of Heilongjiang Province (Fig. 2). It has a total administrative area of 53,100 km^2, a city area of 10,198 km^2, and a built-up area of 428 km^2. By the end of 2015, Harbin had a total population exceeding 5.49 million, with 5403 km^2 of farmland and 135.14 km^2 of urban green space. The per capita public green space was only 9.5 m^2. Harbin experiences a mid-temperate climate, with an annual average temperature of 4.7 °C (2015) and distinct seasonal variations. From November to February, the monthly average temperature remains below 0 °C, with seasonal temperature differences reaching almost 60 °C—ranging from 28 °C in summer to −24 °C in winter. During winter, vegetation coverage is nearly non-existent. According to the updated Köppen–Geiger climate classification (Beck et al., 2020), Harbin falls within a cold climate zone with hot summers and dry winters, where the warmest month's temperature exceeds 22 °C while the coldest monthly mean temperature falls below 0 °C. In this study, in order to minimize the impacts of cloud coverage on the quality of images and considering available of data, the Landsat series remote sensing images (spatial resolution 30 m) were downloaded from the U.S. Geological Survey website. MODIS data are from NASA website (https://search.earthdata.nasa.gov/search/).

3. Results

3.1. The temporal and spatial characteristics of the urban heat island effects

Using the radiative transfer equation method (Eqs. (1)–3), this study retrieves the summer and winter diurnal LST of Harbin City from 2000 to 2020. The LST at night are also obtained by MODIS data. Figs. 3–6 show the results and distribution histograms of the daytime and nighttime LST in summer and winter, respectively. As shown in Fig. 3 and 4, in general, the extent of high-temperature areas in summer expands gradually from 2000 to 2020. The most remarkable temperature increase occurs between 2015 and 2020, as observed in the temperature distribution on the histograms (upper left corner of Figures). The occurrence frequency of temperatures above 34 °C increases from 13,789 to 139,163, with a growth of 125,374 at day. The total land area with nighttime LST more than 24 °C also expand by 710 km^2 from 2015 to 2020. The higher LST value at daytime concentrates on central part of Harbin City where usually undergoes more heat release and absorption. While it comes to central areas and water bodies at night. This is because of massive heat radiation storage during daytime but slower cooling and evaporation rates for water bodies and built-up areas during nighttime (Steeneveld et al., 2014; R. Wang et al., 2021).

There is a clear fluctuation in Harbin City's winter LST over the 20-year period, as shown in Fig. 5&6. The diurnal mean LST increases from −26.57 °C in 2000 to −18.84 °C in 2005, then drops to −28.68 °C in 2010, before rising again to −16.25 °C in 2020. The nighttime mean LST

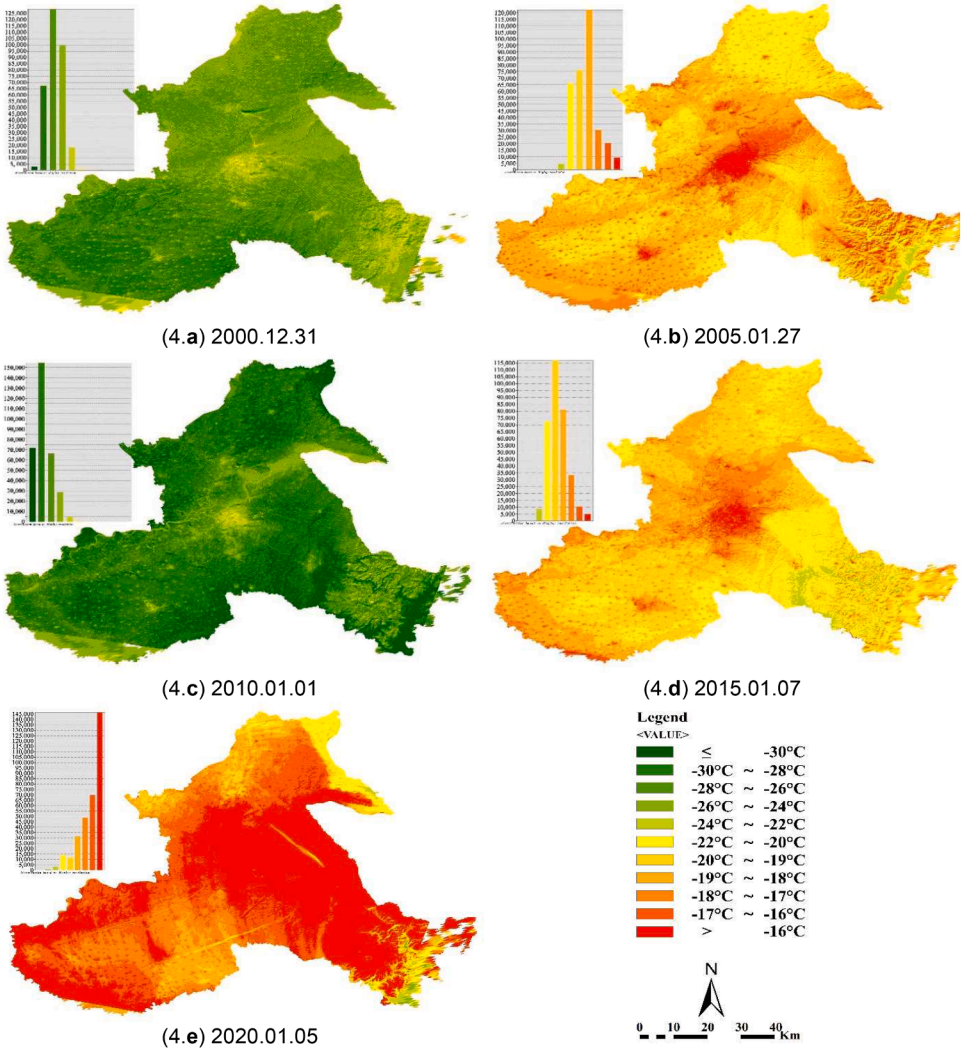

Fig. 5. The LST patterns and distribution histograms of Harbin city in the winter day (2000–2020).

climbs up to-25.68 °C in 2005, then goes back down to −31.50 °C of 2010. After an increase of 7.74 °C in 2005, the nighttime mean LST appears a smaller decrease with 0.51 °C to −24.27 °C in 2020. The histograms on the left of each figures depict clearly the frequency distribution of different LST ranges. For example, for winter daytime in 2020, the highest frequency is observed in the LST range appears at more than −16 °C, followed by −17∼−16 °C. Nearly 146,621 frequency (4588 km^2) have an LST above −16 °C, which is 14,662.1 and 15.7 times of 2000 and 2005, separately. Even though in winter of cold climate area, high temperature phenomenon is enhancing.

According to Table 1, the SUHII of Harbin City shows an overall increase in both summer daytime and nighttime from 2000 to 2020, while it emerges obvious fluctuation in winter (Table 2). When comparing the winter SUHII with the summer SUHII for all study years, it is found that the summer diurnal SUHII (ranging from 1.38 °C to 5.51 °C) is significantly higher than the winter diurnal SUHII (0.52 °C to 1.10 °C). This contradicts the findings of previous studies (García-Cueto et al., 2007; He et al., 2007), in which García-Cueto's study focused on a hot, arid desert climate (BWh) city Mexicali, and He et al.(2007) used very limited number of meteorological stations (673 for whole China). Fig. 7 also illustrates that the UHI effect in summer daytime is stronger than that in winter for cold climates, and more interestingly, higher summer urban heat island effects correspond to lower winter urban heat island effects in that specific study year during daytime.

3.2. Relationship between SUHII and green ration (GIF and NVDI)

In the study, the green infrastructure fraction (Fig. 8) and SUHII are first extracted using 1200 m × 1200 m grids. The Green Infrastructure Fraction (GIF) statistics are derived from LULC classification data (2010) of Second National Land Survey Database in China. Its value is between 0 and 1. The value 0 indicates that the LULC types of the grid are the construction land or other land, while the value 1 demonstrates that the grid is entirely covered by green infrastructures. The middle yellow part in Fig. 8 with sparse green infrastructure cover, belongs to the urban built-up area of Harbin city. Therefore, the 0 value is mainly distributed in these areas.

The current paper establishes linear regression equations between the green infrastructure fraction and SUHII at the grid scale. The results (Fig. 9) indicate that SUHII still shows a negative correlation with the green infrastructure fraction (Weng et al., 2011) in both summer and winter at a significance level of 0.0005. The correlation between SUHII and GIF in winter (with $R = -0.30$ at daytime, and $R = -0.24$ at nighttime) is significantly lower than that in summer daytime (with $R = -0.72$). While the Nighttime SUHII also displays inapparent relevance to GIF. Nevertheless, the linear relationship confirms that an increase in green vegetation can indeed alleviate urban heat island effects, especially for summer daytime.

The study also analyses the correlation between SUHII and NDVI (as a proxy for the green ratio) to determine whether the green

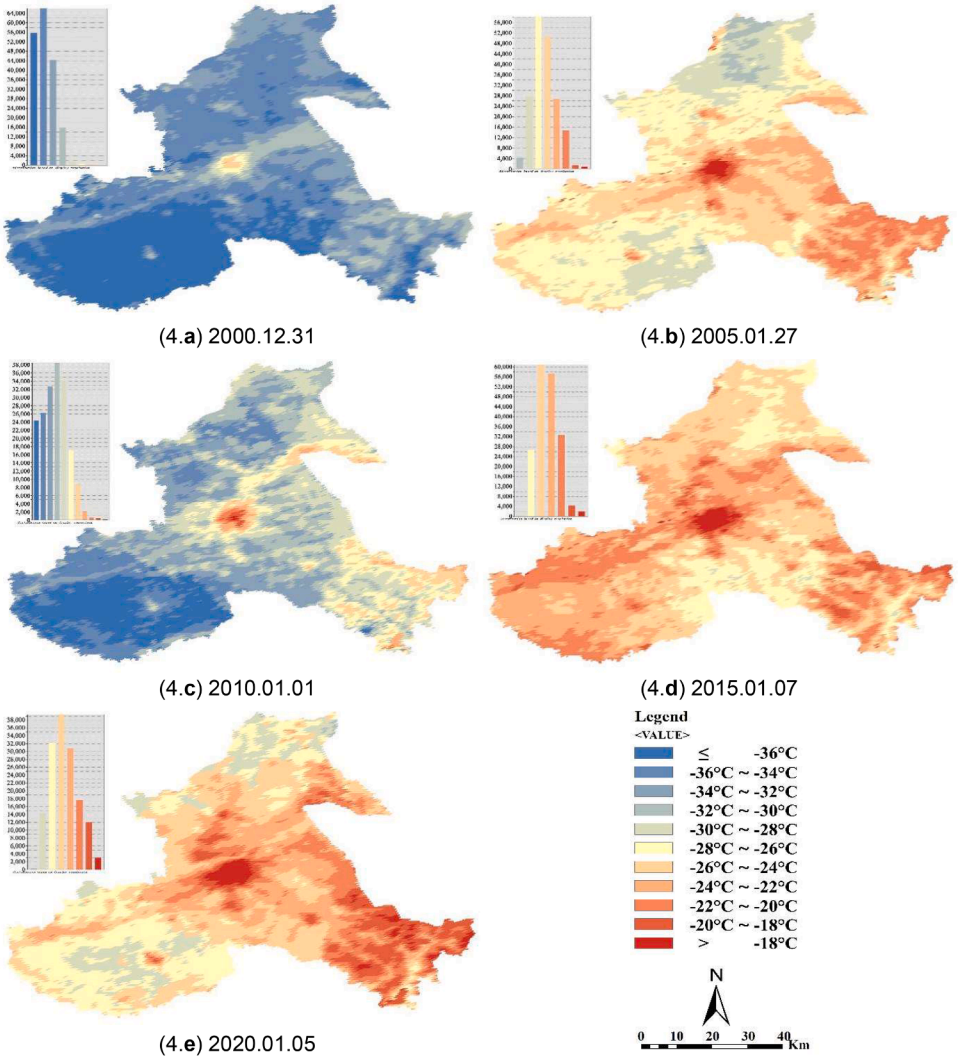

Fig. 6. The LST patterns and distribution histograms of Harbin city in the winter night (2000–2020).

Table 1
The changes of the SUHII for Harbin city in the summer (2000–2020).

Time (Year)	Mean Daytime LST (°C)			Daytime SUHII (°C)	Mean Nighttime LST			Nighttime SUHII (°C)
	Total	Urban	Suburban		Total	Urban	Suburban	
2000	27.77	29.99	27.07	2.92	17.14	17.46	17.04	0.42
2005	26.22	27.27	25.89	1.38	19.05	19.87	18.80	1.07
2010	25.72	27.22	25.24	1.98	16.75	17.83	16.42	1.41
2015	27.44	29.38	26.83	2.55	18.01	18.58	17.82	0.76
2020	33.57	37.76	32.25	5.51	21.74	22.60	21.47	1.13

Table 2
The changes of the SUHII for Harbin city in the winter (2000–2020).

Time (Year)	Mean Daytime LST (°C)			Daytime SUHII (°C)	Mean Nighttime LST			Nighttime SUHII (°C)
	Total	Urban	Suburban		Total	Urban	Suburban	
2000	−26.57	−26.10	−26.72	0.62	−34.92	−33.64	−35.32	1.68
2005	−18.84	−18.18	−19.05	0.87	−25.68	−24.73	−25.98	1.25
2010	−28.68	−28.28	−28.80	0.52	−31.50	−30.28	−31.88	1.6
2015	−19.27	−18.43	−19.53	1.1	−23.76	−23.04	−23.99	0.95
2020	−16.25	−15.62	−16.45	0.83	−24.27	−23.09	−24.64	1.55

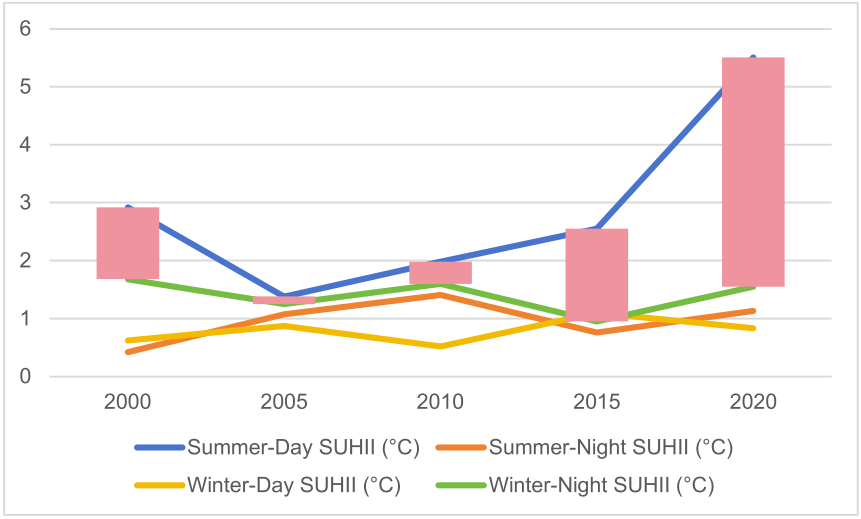

Fig. 7. Yearly and seasonal SUHII Variations.

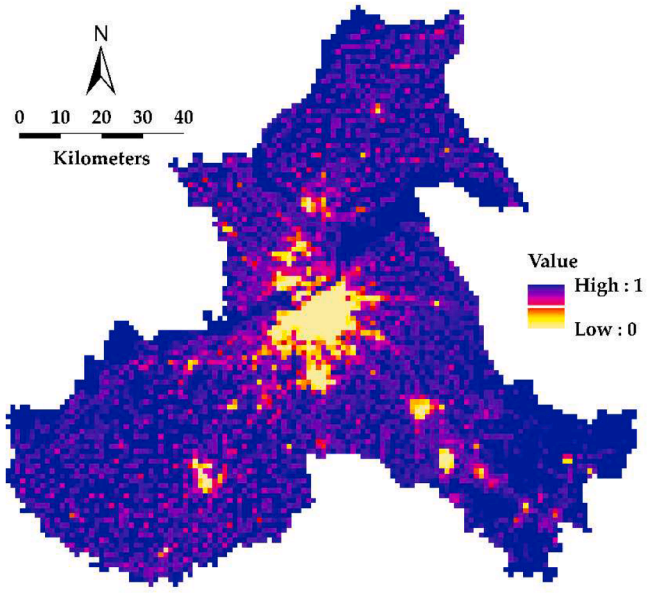

Fig. 8. The distribution pattern of the green infrastructure fraction.

infrastructure fraction index is more effective than NDVI in the study of UHI. Fig. 10 reveals that SUHII is negatively correlated with NDVI in summer but positively correlated in winter. Furthermore, the linear trends between SUHII and NDVI are weaker than those between SUHII and GIF in both summer and winter daytime. Whereas the correlation coefficient between SUHII and NDVI in summer is only −0.36, the coefficient between winter SUHII and NDVI is even lower, at just 0.17. This again indicates that the vegetation fraction is superior to NDVI, as shown in similar studies (Ma et al., 2008; Weng et al., 2004), when investigating the correlation between vegetation cover and UHI at daytime. When it comes to nighttime SUHII in summer, its relevance to vegetation index is just opposite to daytime. Using NDVI as an indicator is better than GIF, and the correlation coefficient shows a superiority of 0.5.

3.3. The results of green retrofitting scenario simulation

Dense urban areas and highly commercial zones are observed to have the highest UHI levels (Mohan et al., 2013; Zandi et al., 2022). In Harbin City, dense urban areas and highly commercial zones are located in Daoli District, Nangang District, and Xiangfang District. Based on LST distribution characteristics in 2010, hot spots are also concentrated within these areas, as shown in Fig. 11. The selected UHI hot spot is characterised by high-density mixed-use building blocks without designated spaces for parks. The building blocks measure 60 m × 60 m, with building heights ranging from around 12 m to 22 m. Currently, the site has only a limited number of street trees and a small roadside green space, and it is situated far from public green spaces. Therefore, this site, shown in Fig. 11, is selected for green retrofitting studies.

For urban green retrofitting planning, we establish three simulation scenarios (Fig. 12): the basic scenario, the improved scenario, and the green scenario. The basic scenario simulates conditions based on the existing green infrastructure fraction (1.6 %). In the improved scenario, only street trees are increased, raising the green infrastructure fraction to 4.3 %. The green scenario builds upon the improved scenario by replacing conventional roofs with green roofs, further increasing the green infrastructure fraction to 30 %.

Using ENVI-met software, this study simulates air temperature at 6:00 am, 2:00 pm, and 8:00 pm under the three scenarios. The simulation results for the three scenarios are presented in Fig. 13 and Table 3. The higher temperature occurs at 2:00 pm, while the temperature distributions at 6:00 am and 8:00 pm are similar. This pattern is broadly consistent with the temporal temperature distribution reported by the meteorological station, which recorded 25 °C at 6:00 am, 28 °C at 2:00 pm and 8:00 pm (weather station data are from https:// en.tutiempo.net/climate). Based on long-term real-time weather statistics for Harbin City, 2:00 PM is typically the hottest time of the day. Furthermore, the National Climatic Data Center estimates that peak temperatures generally occur two to three hours after noon, depending on cloud cover and wind speed variability (Finfrock, 2008). An increase in street tree canopy cover, raising the green infrastructure fraction to 4.3 %, yield no statistically significant decline in air temperature at 1.5 m height compared to the baseline scenario (Fig. 14). At this stage, the highest air temperatures are recorded in streets and courtyard spaces enclosed by buildings at afternoon, followed by the buildings themselves. In the morning, buildings themselves are of lower temperature than other areas, while building areas turn into hottest among the site at night. When green roofs replace conventional roofs, increasing the green infrastructure fraction to 30 %, air temperature exhibits a slight overall reduction. Fig. 14 illustrates that the temperature in the simulated area decreases by approximately 0~9.41 °C if adding the use of green roofs. The most significant effect of green roofs on temperature manifest in the early morning with biggest reduction of 9.41 °C. These findings indicate that air temperature at 1.5 m above ground level begins to decrease only once the green infrastructure fraction reaches a certain threshold—30 %

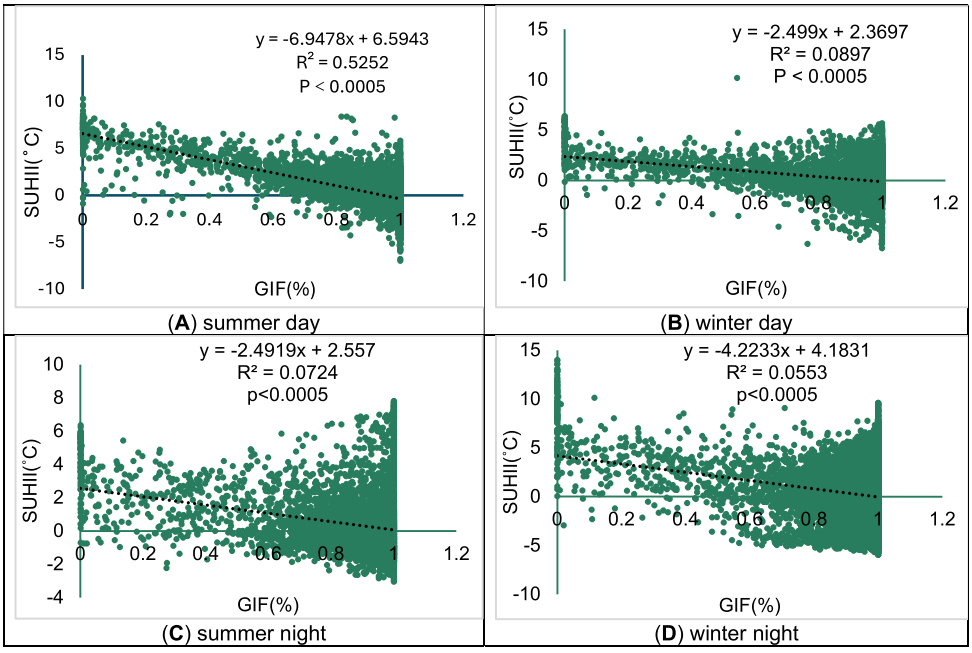

Fig. 9. The linear regression results of the SUHII and GIF at 1.2 km by 1.2km.

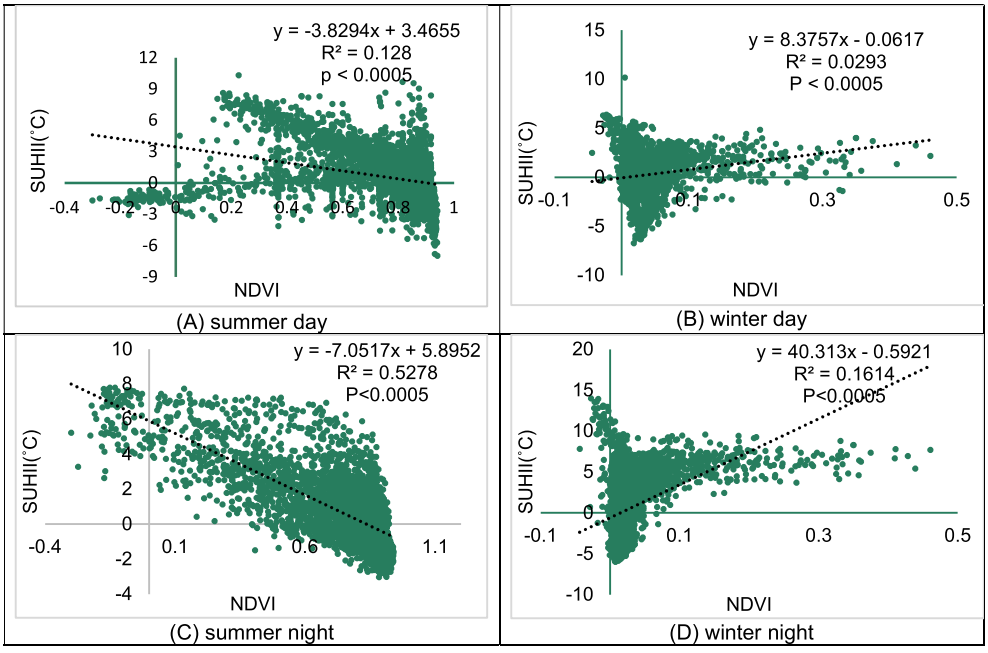

Fig. 10. The linear regression results of the SUHII and NDVI at 1.2 km by 1.2km.

in this study. Therefore, a strategically measured increase in green roofs in densely populated urban areas can serve as a viable approach to mitigating the urban heat island (UHI) effect as confirmed in related studies (Jamei et al., 2019; Liu et al., 2021).

3.4. Population decline, UHI and, urban green infrastructure

Research shows that rapid urbanisation has significant impacts on the urban heat island (UHI) effect (Mathew et al., 2017; Singh et al., 2017; Son et al., 2017). However, there is very little research on the UHI effects of depopulation in cities. Depopulation does not necessarily lead to a reduction in construction land or an increase in green infrastructure; instead, it has been associated with a significant rise in UHI effects, as demonstrated in Section 3.2. We introduced a regression model to examine the relationship between SUHII and various socioeconomic indicators, including population density, GDP, and land use/land cover (LULC) changes. The results as shown in Table 4 indicate that over 67 % of the variation in SUHII can be explained by these socioeconomic factors. However, the regression model fails to pass standard diagnostic tests, suggesting that the influence of these socioeconomic variables on SUHII in Harbin is statistically uncertain. Based on prior feature analysis of seasonal SUHII during both day and night, only diurnal SUHII was found to be meaningful for assessing the impact of socioeconomic factors on urban heat islands (UHI). Consequently, a robust regression model—designed to mitigate the influence of outliers—was employed. The results suggest that SUHII increases as population density decreases,

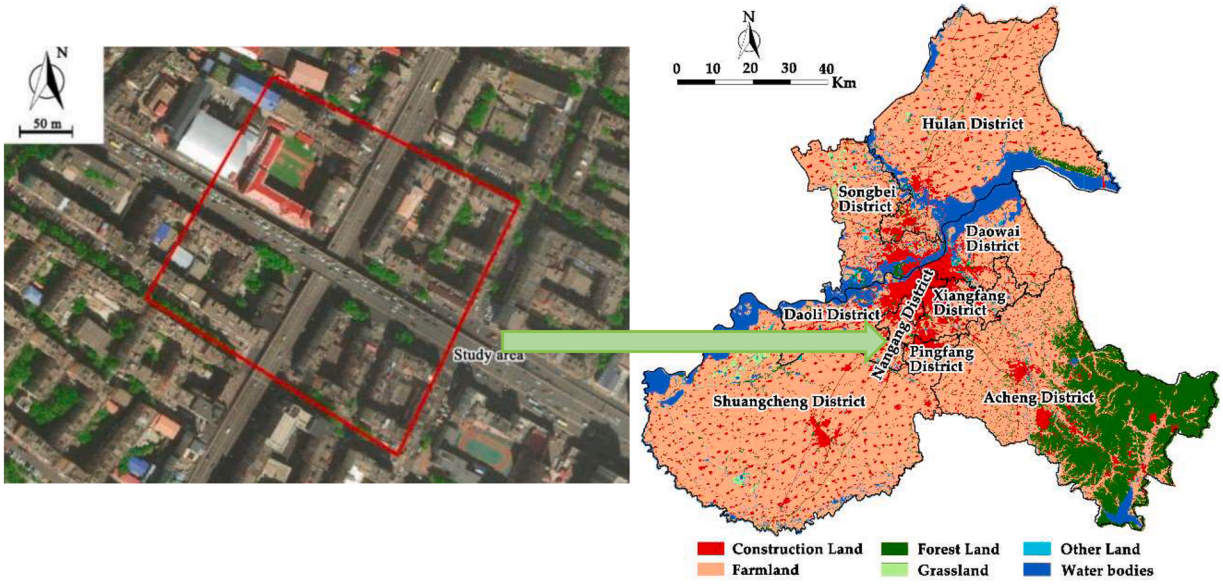

Fig. 11. Green Retrofitting Study Site.

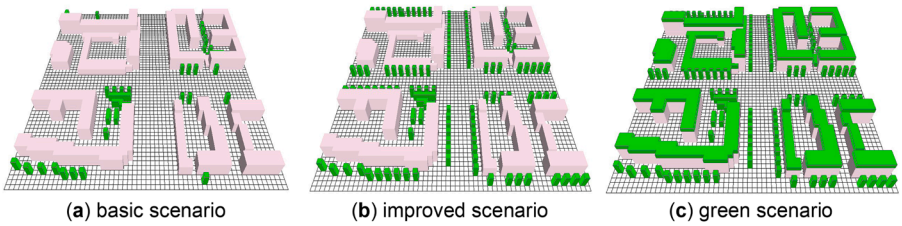

Fig. 12. Three green retrofitting scenarios of the ENVI-met model. (60mX60m).

whereas it tends to decline with reductions in GDP and the Green Infrastructure Fraction (GIF). However, current analysis was limited by a lack of detailed and reliable geospatial data on these specific urban elements. This constraint prevented us from modelling their direct thermal contributions at finer spatial scales. Nevertheless, the results in Table 4 indicate intensified urban heat island (UHI) effect despite population decline at the macro city level.

4. Discussion

This study analysed the temporal and spatial characteristics of the Urban Heat Island Effects, and assessed the relationship between green infrastructure and SUHI under the scale of grid. To further investigate the influence of green infrastructure on UHI, the study simulated air temperature changes under different green infrastructure fraction scenarios, and also explored the impact of key socioeconomic indicators on SUHII. The key findings and innovations of this study are as follows::

- Vegetation-UHI Dynamics in Cold Climates: It provides a detailed spatiotemporal case study demonstrating a strong negative correlation between green infrastructure fraction (GIF) and surface urban heat island intensity (SUHII) in both summer and winter, filling a gap in understanding year-round UHI mitigation in cold-climate cities.
- *Re*-evaluation of Seasonal UHI Patterns: By showing that summer daytime SUHII exceeds winter values contradicting previous studies. It challenges existing assumptions and calls for regionally nuanced seasonal UHI analyses.
- Improved Vegetation Metrics: The study identifies GIF as a potentially more accurate and stable metric than NDVI for quantifying urban vegetation, suggesting a methodological shift in how vegetation cover is assessed in UHI studies.
- Practical UHI Mitigation Strategies: It demonstrates the effectiveness of green roofs in lowering air temperatures, encouraging planners to consider diversified green infrastructure strategies tailored to local conditions.
- Urban Greening in Shrinking Cities: It reveals that UHI effects can intensify despite population decline, due to continued urban expansion and loss of vegetation, highlighting an overlooked need to integrate greening policies into planning for shrinking cities.

In this study, it is found that GIF is a better than NDVI when investigating the correlation between vegetation cover and UHI (Ma et al., 2008; Weng et al., 2004), except for the summer nighttime. NDVI only represents vegetation greenness and cannot distinguish vegetation types (such as grasslands and trees). For instance, under high summer temperatures, low grasslands (with probably higher NDVI values) have limited cooling effect than green spaces dominated by trees (Skelhorn, Lindley & Levermore 2014; Sodoudi et al. 2018), resulting in a weaker correlation between NDVI and SUHII. Moreover, the NDVI value of water bodies is below zero, it also cannot be distinguished from snow and clouds (Saravanan et al., 2018). However, GIF reflects the overall proportion of green spaces (grasslands, water bodies, forests, etc.) in the city, including the structural integrity and ecological functions of vegetation, which can better influence the change of SUHII (Chen et al. 2022; Rakoto et al. 2021). But in Harbin's winter, vegetation enters a dormant period. At this point, green spaces in GIF loses its cooling function, while the NDVI can still reflect limited greenness of evergreen vegetation. Therefore, it is important to be more cautious when using NDVI in UHI and urban green research and policy analysis.

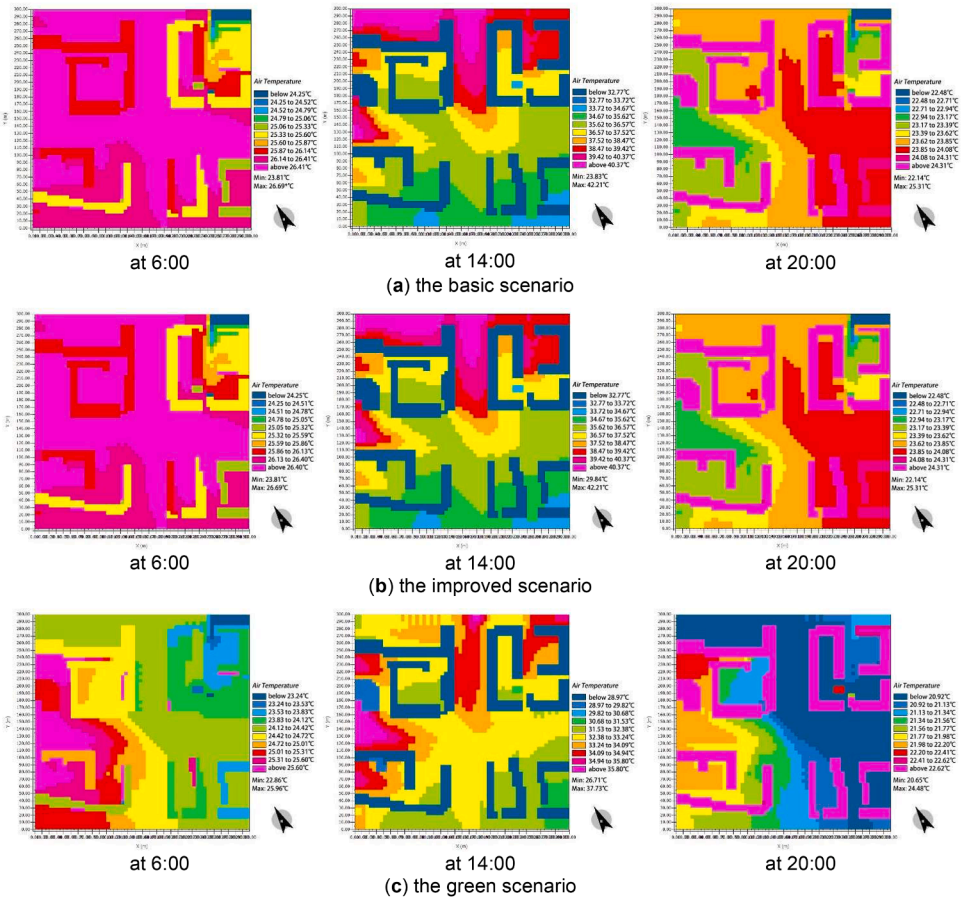

Fig. 13. The simulated results of the air temperature change with the green infrastructure fraction.

Table 3
The percentage of temperature reduction in three scenarios.

Scenarios	Setting	GIF	Simulated temperature at different time			T changes compared to a
				Min	Max	
a) Basic scenario	Limited green vegetation	1.6 %	6 am	23.81 °C	26.69 °C	—
			2 pm	23.83 °C	42.21 °C	
			8 pm	22.14 °C	25.31 °C	
b) Improved scenario	Increasing street trees	4.3 %	6 am	23.81 °C	26.69 °C	0 ~ +0.01 °C
			2 pm	29.84 °C	42.21 °C	−0.03 ~ +0.05 °C
			8 pm	22.14 °C	25.31 °C	0 °C
c) Green scenario	Increasing green roofs and street trees	30 %	6 am	22.86 °C	25.96 °C	+0.66 ~ −2.42 °C
			2 pm	26.71 °C	37.73 °C	−2.10~ −9.41 °C
			8 pm	20.65 °C	24.48 °C	−0.77 ~ −3.18 °C

Note: "+" means the increase in temperature; "-" means the decrease in temperature.

Based on the simulation of year-round thermal regulation potential of green roofs in cold climates, practical green roof policies are needed to encourage their installation (Clar & Steurer 2023; Liberalesso et al. 2020), particularly in areas with limited open space for street trees. However, appropriate fiscal support must be provided for economically disadvantaged neighborhoods. Additionally, practical characteristics of buildings, such as the structural suitability of existing constructions need to be carefully assessed.

The SUHII in Harbin continues to rise despite declining population density, primarily due to urban spatial development strategies and planning orientations influenced by specific institutional frameworks and policy directives (Harbin Municipal People's Government, 2006, 2004). Urban development policies in Harbin have often prioritised economic efficiency, promoting increased GDP output with reduced labour input, which has led to urban expansion and a growth in built-up areas despite a declining urban population and diminishing green spaces. As a result, surface urban heat island intensity (SUHII) in Harbin continues to rise, primarily driven by spatial development strategies and planning orientations shaped by institutional frameworks and policy directives (Harbin Municipal People's Government, 2004, 2006). For instance, policies such as the "Relocation of Secondary Industries and Tertiary Industry Development" (Tui er Jin San), the Harbin New District Development Policy, and population decentralisation programmes have effectively redistributed the population from traditional high-density core urban areas, often mixed-use industrial and residential zones, to newly developed peripheral areas. While this redistribution has contributed to a city-wide decrease in population density, it is paradoxically associated with a rise in SUHII due to several interrelated factors. Firstly, the vacated core areas have increasingly transitioned to energy-intensive tertiary sectors (e.g. commercial, office, financial services), which, despite declining residential populations, drive anthropogenic heat emissions and increase the extent of impervious surfaces, thus sustaining or intensifying UHI effects. Second, outward spatial expansion has led to the proliferation of newly built-up areas at the cost of natural vegetation and green spaces. These new developments often lack mature green infrastructure, particularly tree canopy cover with

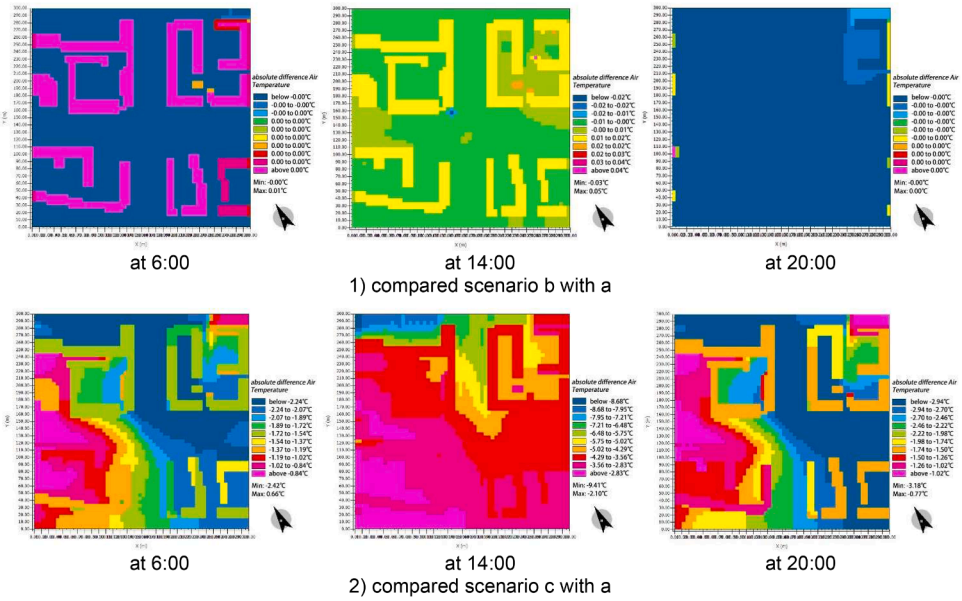

Fig. 14. The level of temperature reduction when comparing two different scenarios.

Table 4
The changes of the population density and land use for Harbin city (2000–2020).

	Population Density (people/km2)	GDP (100 million yuan)	LULC Changes (%)		Summer SUHII (°C)		Winter SUHII (°C)	
			GIF	Built-up land	Daytime	Nighttime	Daytime	Nighttime
2000	539.5	682.0	92.7	7.3	2.92	0.42	0.62	1.68
2005	534.7	678.5	92.4	7.6	1.38	1.07	0.87	1.25
2010	666.8	2578.7	88.9	11.1	1.98	1.41	0.52	1.6
2015	662.5	4129.5	91	9.0	2.55	0.76	1.1	0.95
2020	543.0	3972.4	88.3	11.7	5.51	1.13	0.83	1.55

Data source: Harbin Statistics Yearbook.

high evapotranspiration capacity, making them vulnerable to becoming new UHI hotspots. Additionally, Harbin's land finance and development model continues to favour rapid outward expansion over ecologically sensitive urban renewal. This approach, prioritising development speed over environmentally refined strategies, further exacerbates the challenges associated with urban heat island effects. These findings highlight the urgent need for comprehensive urban re-greening strategies in post-industrial cities undergoing population decline. The implementation of large-scale green infrastructure initiatives could play a vital role in mitigating UHI impacts, enhancing environmental quality, and strengthening urban resilience in the face of socio-economic and ecological transitions (De la Sota et al. 2019; Rayan, Gruehn & Khayyam 2021; Saaroni et al. 2018; Ugochukwu Kanayo Ashinze et al. 2024).

The study acknowledged the limitations of using remote sensing data, such as the precision of data fusion and gaps due to clouds. Because of a lack of reliable data on biophysical vegetation structure parameters (e.g., leaf area index and heights), vacant buildings and underutilised grey infrastructure, this study does not analyse the role of these elements in urban heat dynamics too. Future research should address these limitations and explore interim greening strategies such as green roofs, temporary green lots, and community gardens be explored as adaptive solutions in future urban climate resilience policies. The substantial variations in SUHII at the same GIF can be attributed to several factors. Firstly, the influence of surrounding cells plays a crucial role, warranting further investigation. Secondly, different types of green infrastructure (GI), such as water bodies, bare land, or irrigated areas, exhibit varying cooling effects on land surface temperature (LST), which should be explored in future studies.

5. Conclusion

This study developed a comprehensive urban greening decision-making framework to explore the relationship between urban heat islands (UHI) and green infrastructure fraction (GIF), and to support green retrofitting efforts. The framework integrates multi-source data and computational modelling techniques, enabling evidence-based decision-making in UHI mitigation. The main conclusions are following:

1) A detailed temporal and spatial case study of Harbin revealed a significant negative correlation between GIF and SUHII, demonstrating that increased vegetation cover effectively reduces UHI effects in both summer and winter.
2) Summer daytime SUHII values were consistently higher than winter values, contradicting some previous findings for cold-climate cities.
3) GIF was proved to be a more reliable measure than NDVI for assessing urban vegetation cover. The study's findings support the use of green infrastructure fraction as a proxy for vegetation coverage and highlight the need for further investigation into the factors contributing to LST changes.
4) The study also demonstrated the effectiveness of green roofs in reducing air temperatures, suggesting that urban planners should explore various types and proportions of green infrastructure to optimize UHI mitigation.
5) Despite a declining population, Harbin experienced increased built-up area and UHI effects, highlighting the critical need to prioritize urban greening initiatives even in shrinking cities.

In conclusion, this study provides valuable insights into the seasonal

and temporal characteristics of SUHI in Harbin and the relationship between SUHII and green infrastructure fraction. The findings underscore the importance of increasing green infrastructure to mitigate UHI effects, particularly in cold-climate cities. Urban planners, architects, and designers should prioritize the preservation and expansion of green infrastructures to enhance urban resilience and sustainability.

However, there is a gap in detailed geospatial datasets, such as vegetation height, leaf area index, or building usage types. This restricts precise modelling of thermal contributions of different types of green and grey infrastructure. Future research should continue to explore the role of different types of green infrastructures and their biophysical vegetation parameters (such as LAI and height of trees) in improving thermal comfort and mitigating UHI. Although socioeconomic variables (GDP, population density, land use) explain part of the variation in SUHII, the relationships remain statistically uncertain, indicating a need for richer datasets and non-linear models to fully capture urban thermal responses.

Funding

This work was supported by the Tianjin Municipal Education Commission Research Program [grant number 2023SK074;grant name: Identification and Optimization Strategies of Blue-Green Space Types in Tianjin Based on the “Cooling Potential-Benefit”].

CRediT authorship contribution statement

Yujing Bai: Writing – original draft, Visualization, Software, Project administration, Methodology, Funding acquisition, Data curation, Conceptualization. **Yangang Xing:** Writing – review & editing, Validation, Supervision, Methodology, Conceptualization.

Declaration of competing interest

We have nothing to declare.

Data availability

Data will be made available on request.

References

Amiri, R., Weng, Q., Alimohammadi, A., & Alavipanah, S. K. (2009). Spatial-temporal dynamics of land surface temperature in relation to fractional vegetation cover and land use/cover in the Tabriz urban area, Iran. *Remote Sensing of Environment, 113* (12), 2606–2617. https://doi.org/10.1016/j.rse.2009.07.021

Bai, Y., Guo, R., & Xing, Y. (2018). Relationship between urban heat island and green infrastructure fraction in Harbin. In N. Chrysoulakis, T. Erbertseder, & Y. Zhang (Eds.), *Remote sensing technologies and applications in urban environments iii: 10793. Remote sensing technologies and applications in urban environments iii* (pp. 1–10). SPIE. https://doi.org/10.1117/12.2501937.

Barsi, J. A., Barker, J. L., & Schott, J. R. (2003). An atmospheric correction parameter calculator for a single thermal band earth-sensing instrument. In *, 00. IEEE International Geoscience and Remote Sensing Symposium 2003* (pp. 2–4). https://doi.org/10.1109/IGARSS.2003.1294665

Barsi, Julia A., Schott, J.R., Palluconi, F.D., .& Hook, S.J. (.2005). *Validation of a web-based atmospheric correction tool for single thermal band instruments*. 58820E. 10.1117/12.619990.

Bass, B., Krayenhoff, S., Martilli, A., & Stull, R. (2002). Mitigating the urban heat island with green roof infrastructure. In *Urban Heat Island Summit: Mitigation of and Adaptation to Extreme Summer Heat, 2002, Toronto, 1-4 May 2002* (p. 10).

Beck, H. E., Zimmermann, N. E., McVicar, T. R., Vergopolan, N., Berg, A., & Wood, E. F. (2020). Publisher Correction: Present and future Köppen-Geiger climate classification maps at 1-km resolution. *Scientific Data, 7*(1), 274. https://doi.org/10.1038/s41597-020-00616-w

Chen, H. Y., Deng, Q. L., Zhou, Z., Ren, Z. G., & Shan, X. F. (2022). Influence of land cover change on spatio-temporal distribution of urban heat island -a case in Wuhan main urban area. *Sustainable Cities and Society*, 79. https://doi.org/10.1016/j.scs.2022.103715

Chen, X. L., Zhao, H. M., Li, P. X., & Yin, Z. Y. (2006). Remote sensing image-based analysis of the relationship between urban heat island and land use/cover changes. *Remote Sensing of Environment, 104*(2), 133–146. https://doi.org/10.1016/j.rse.2005.11.016

Clar, C., & Steurer, R. (2023). Climate change adaptation with green roofs: Instrument choice and facilitating factors in urban areas. *Journal of Urban Affairs, 45*(4), 797–814. https://doi.org/10.1080/07352166.2021.1877552

Cui, Y., & Foy, B. De (2012). Seasonal Variations of the Urban Heat Island at the Surface and the Near-Surface and Reductions due to Urban Vegetation in Mexico City. *Journal of Applied Meteorology and Climatology, 51*(5), 855–868. https://doi.org/10.1175/JAMC-D-11-0104.1

De la Sota, C., Ruffato-Ferreira, V. J., Ruiz-García, L., & Alvarez, S. (2019). Urban green infrastructure as a strategy of climate change mitigation. A case study in northern Spain. *Urban Forestry & Urban Greening, 40*, 145–151. https://doi.org/10.1016/j.ufug.2018.09.004

Du, H. L., Zhan, W. F., Liu, Z. H., Li, J. F., Li, L., Lai, J. M., Miao, S. Q., Huang, F., Wang, C. G., Wang, C. L., Fu, H. Y., Jiang, L., Hong, F. L., & Jiang, S. D. (2021). Simultaneous investigation of surface and canopy urban heat islands over global cities. *ISPRS Journal of Photogrammetry and Remote Sensing, 181*, 67–83. https://doi.org/10.1016/j.isprsjprs.2021.09.003

EARTH OBSERVING SYSTEM. (2019). NDVI FAQ: All you need to know about NDVI. https://eos.com/blog/ndvi-faq-all-you-need-to-know-about-ndvi/.

Ely, M., & Pitman, S. (2014). *Green infrastructure: Life support for human habitats*. Botanic Gardens of Adelaide, Department of Environment, Water and Natural Resources. http://apo.org.au/node/135761.

Feyisa, G. L., Dons, K., & Meilby, H. (2014). Efficiency of parks in mitigating urban heat island effect: An example from Addis Ababa. *Landscape and Urban Planning, 123*, 87–95. https://doi.org/10.1016/j.landurbplan.2013.12.008

Finfrock, D. (2008). NBC 5 Weather: What is the Hottest Time of the Day?. https://nbc5weather.wordpress.com/2008/07/28/what-is-the-hottest-time-of-the-day/.

García-Cueto, O. R., Jáuregui-Ostos, E., Toudert, D., & Tejeda-Martinez, A. (2007). Detection of the urban heat island in Mexicali, B. C., México and its relationship with land use. *Atmósfera, 20*(2), 111–131.

Gong, P., Liang, S., Carlton, E. J., Jiang, Q., Wu, J., Wang, L., & Remais, J. V. (2012). Urbanisation and health in China. *The Lancet, 379*(9818), 843–852. https://doi.org/10.1016/S0140-6736(11)61878-3

Greene, C. S., & Kedron, P. J. (2018). Beyond fractional coverage: A multilevel approach to analyzing the impact of urban tree canopy structure on surface urban heat islands. *Applied Geography, 95*, 45–53. https://doi.org/10.1016/j.apgeog.2018.04.004

Grimm, N. B., Faeth, S. H., Golubiewski, N. E., Redman, C. L., Wu, J., Bai, X., Briggs, J. M., Grimm, N. B., Faeth, S. H., Golubiewski, N. E., Redman, C. L., Wu, J., Bal, X., & Briggs, J. M. (2008). Global Change and the Ecology of Cities. *Science (New York, N.Y.), 319*(5864), 756–760. https://doi.org/10.1126/science.1150195

Hales, S. (2016). *Climate Change 2007: Impacts, adaptation and vulnerability* (Issue (January)).

Harbin Municipal People’s Government. (2006). Overall planning of Harbin Metropolitan area (2005-2020). 1–11.

Harbin Municipal People’s Government. (2004). The master plan of Harbin City (2004-2020).1-247. Hasanlou, M., & Mostofi, N. (2015). Investigating Urban Heat Island Estimation and Relation between various land cover indices in Tehran City using Landsat 8 Imagery. In *The 1st International Electronic Conference Remote Sensing*. https://www.researchgate.net/profile/Nikrouz_Mostofi/publication/285045741_Investigating_Urban_Heat_Island_Estimation_and_Relation_between_Various_Land_Cover_Indices_in_Tehran_City_Using_Landsat_8_Imagery/links/565b00e208ae4988a7ba69c9/Investigating-Urban.

He, J. F., Liu, J. Y., Zhuang, D. F., Zhang, W., & Liu, M. L. (2007). Assessing the effect of land use/land cover change on the change of urban heat island intensity. *Theoretical and Applied Climatology, 90*(3–4), 217–226. https://doi.org/10.1007/s00704-006-0273-1

Hu, Y., & Jia, G. (2010). Influence of land use change on urban heat island derivedfrom multi-sensor data. *International Journal of Climatology, 30*(9), 1382–1395. https://doi.org/10.1002/joc.1984

Jamei, Y., Rajagopalan, P., & Sun, Q.(Chayn) (2019). Spatial structure of surface urban heat island and its relationship with vegetation and built-up areas in Melbourne, Australia. *Science of The Total Environment, 659*, 1335–1351. https://doi.org/10.1016/J.SCITOTENV.2018.12.308

Jenerette, G. D., Harlan, S. L., Brazel, A., Jones, N., Larsen, L., & Stefanov, W. L. (2007). Regional relationships between surface temperature, vegetation, and human settlement in a rapidly urbanizing ecosystem. *Landscape Ecology, 22*(3), 353–365. https://doi.org/10.1007/s10980-006-9032-z

Jiménez-Muñoz, J. C. (2003). A generalized single-channel method for retrieving land surface temperature from remote sensing data. *Journal of Geophysical Research, 108* (D22), 4688. https://doi.org/10.1029/2003JD003480

Jin, M., Dickinson, R. E., & Zhang, D. L. (2005). The footprint of urban areas on global climate as characterized by MODIS. *Journal of Climate, 18*(10), 1551–1565. https://doi.org/10.1175/JCLI3334.1

Jusuf, S. K., Wong, N. H., Hagen, E., Anggoro, R., & Hong, Y. (2007). The influence of land use on the urban heat island in Singapore. *Habitat International, 31*(2), 232–242. https://doi.org/10.1016/j.habitatint.2007.02.006

Kan, Z., Liu, C., & Li, Z. (2016). Retrieval of land surface temperature based on Landsat-8 thermal infrared data and heat island effect analysis over the Taihu Lake region. *Journal of East China Normal University(Natural Science, 4*, 129–138. https://doi.org/10.3969/j.issn.1000-5641.2016.04.015, 168.

Kanayo Ashinze, Ugochukwu, Aibhamen Edeigba, Blessing, Akpan Umoh, Aniekan, Biu, Preye Winston, & Daraojimba, Andrew Ifesinachi (2024). Urban green infrastructure and its role in sustainable cities: A comprehensive review. *World Journal of Advanced Research and Reviews, 21*(2), 928–936. https://doi.org/10.30574/wjarr.2024.21.2.0519

Kawamoto, Y. (2016). Effect of Urbanization on the Urban Heat Island in Fukuoka-Kitakyushu Metropolitan Area, Japan. *Procedia Engineering, 169*(9), 224–231. https://doi.org/10.1016/j.proeng.2016.10.027

Lehmann, S. (2014). Low carbon districts: Mitigating the urban heat island with green roof infrastructure. *City, Culture and Society, 5*(1), 1–8. https://doi.org/10.1016/j.ccs.2014.02.002

Li, L., & Zha, Y. (2019). Satellite-Based Spatiotemporal Trends of canopy urban heat islands and associated drivers in China's 32 Major Cities. *Remote sensing, 11*(1). https://doi.org/10.3390/rs11010102

Li, X., Zhou, W., & Ouyang, Z. (2013). Relationship between land surface temperature and spatial pattern of greenspace: What are the effects of spatial resolution? *Landscape and Urban Planning, 114*, 1–8. https://doi.org/10.1016/j.landurbplan.2013.02.005

Li, Y. Y., Zhang, H., & Kainz, W. (2012). Monitoring patterns of urban heat islands of the fast-growing Shanghai metropolis, China: Using time-series of Landsat TM/ETM+ data. *International Journal of Applied Earth Observation and Geoinformation, 19*(1), 127–138. https://doi.org/10.1016/j.jag.2012.05.001

Li, Y., Zhang, Y., Wu, Q., Xue, R., Wang, X., Si, M., & Zhang, Y. (2023). Greening the concrete jungle: Unveiling the co-mitigation of greenspace configuration on PM2.5 and land surface temperature with explanatory machine learning. *Urban Forestry & Urban Greening, 88*, Article 128086. https://doi.org/10.1016/j.ufug.2023.128086

Liberalesso, T., Oliveira Cruz, C., Matos Silva, C., & Manso, M. (2020). Green infrastructure and public policies: An international review of green roofs and green walls incentives. *Land Use Policy, 96*, Article 104693. https://doi.org/10.1016/j.landusepol.2020.104693

Liu, Z., Cheng, W., Jim, C. Y., Morakinyo, T. E., Shi, Y., & Ng, E. (2021). Heat mitigation benefits of urban green and blue infrastructures: A systematic review of modeling techniques, validation and scenario simulation in ENVI-met V4. In *Building and environment, 200*. Elsevier Ltd, Article 107939. https://doi.org/10.1016/j.buildenv.2021.107939

Luber, G., & McGeehin, M. (2008). Climate Change and Extreme Heat Events. *American Journal of Preventive Medicine, 35*(5), 429–435. https://doi.org/10.1016/j.amepre.2008.08.021

Ma, W., Chen, Y., Zhou, J., & Gong, A. (2008). Quantitative Analysis of Land Surface Temperature-Vegetation Indexes Relationship Based on Remote Sensing. *The International Archives of the Photogrammetry,Remote Sensing and Spatial Information Sciences, XXXVII*(Part B6b), 261–264. http://citeseerx.ist.psu.edu/viewdoc/download?doi=10.1.1.184.2936&rep=rep1&type=pdf.

Maimaitiyiming, M., Ghulam, A., Tiyip, T., Pla, F., Latorre-Carmona, P., Halik, Ü., Sawut, M., & Caetano, M. (2014). Effects of green space spatial pattern on land surface temperature: Implications for sustainable urban planning and climate change adaptation. *ISPRS Journal of Photogrammetry and Remote Sensing, 89*, 59–66. https://doi.org/10.1016/j.isprsjprs.2013.12.010

Mathew, A., Khandelwal, S., & Kaul, N. (2017). Investigating spatial and seasonal variations of urban heat island effect over Jaipur city and its relationship with vegetation, urbanization and elevation parameters. *Sustainable Cities and Society, 35*, 157–177. https://doi.org/10.1016/j.scs.2017.07.013

Ministry of Land and Resources of the People's Republic of China. (2013). *Communiqué on the Major Data of the Second National Land Survey*. Beijing: Ministry of Land and Resources.

Mohan, M., Kikegawa, Y., Gurjar, B. R., Bhati, S., & Kolli, N. R. (2013). Assessment of urban heat island effect for different land use-land cover from micrometeorological measurements and remote sensing data for megacity Delhi. *Theoretical and Applied Climatology, 112*, 647–658. https://doi.org/10.1007/s00704-012-0758-z

Naumann, S., Davis, M., Kaphengst, T., Pieterse, M., & Rayment, M. (2011). *Final report to the European Commission, DG Environment, Contract no.070307/2010/577182/ETU/F.1*. Ecologic institute and GHK Consulting.

Oke, T. R. (1973). City size and the urban heat island. *Atmospheric Environment Pergamon Pres, 7*, 769–779. https://doi.org/10.1016/0004-6981(73)90140-6

Patz, J. A., Campbell-Lendrum, D., Holloway, T., & Foley, J. A. (2005). Impact of regional climate change on human health. *Nature, 438*(7066), 310–317. https://doi.org/10.1038/nature04188

Qin, Z., Li, W., Xu, B., Chen, Z., & Liu, J. (2004). The estimation of land surface emissivity for Landsat TM6. *Remote Sensing for Land&Resources, 3*, 28–32. https://doi.org/10.6046/gtzyyg.2004.03.07. ,36,41.

QIU, G., yu, L. I., yong, H., ZHANG, Q.tao, CHEN, W., LIANG, X.jian, & LI, X.ze (2013). Effects of Evapotranspiration on Mitigation of Urban Temperature by Vegetation and Urban Agriculture. *Journal of Integrative Agriculture, 12*(8), 1307–1315. https://doi.org/10.1016/S2095-3119(13)60543-2

Rakoto, P. Y., Deilami, K., Hurley, J., Amati, M., & Sun, Q.(Chayn) (2021). Revisiting the cooling effects of urban greening: Planning implications of vegetation types and spatial configuration. *Urban Forestry & Urban Greening, 64*, Article 127266. https://doi.org/10.1016/j.ufug.2021.127266

Rayan, M., Gruehn, D., & Khayyam, U. (2021). Green infrastructure indicators to plan resilient urban settlements in Pakistan: Local stakeholder's perspective. *Urban Climate, 38*, Article 100899. https://doi.org/10.1016/J.UCLIM.2021.100899

Reid, W. W. V. (1998). Biodiversity hotspots. *Trends in Ecology & Evolution, 13*(7), 275–280. https://doi.org/10.1016/S0169-5347(98)01363-9

Saaroni, H., Amorim, J. H., Hiemstra, J. A., & Pearlmutter, D. (2018). Urban Green Infrastructure as a tool for urban heat mitigation: Survey of research methodologies and findings across different climatic regions. *Urban Climate, 24*, 94–110. https://doi.org/10.1016/j.uclim.2018.02.001

Saravanan, S., Jegankumar, R., Selvaraj, A., Jacinth Jennifer, J., & Parthasarathy, K. S. S. (2018). Utility of Landsat Data for Assessing Mangrove Degradation in Muthupet Lagoon, South India. *Coastal zone management: Global perspectives, regional processes, local issues* (pp. 471–484). Elsevier. https://doi.org/10.1016/B978-0-12-814350-6.00020-3

Singh, P., Kikon, N., & Verma, P. (2017). Impact of land use change and urbanization on urban heat island in Lucknow city, Central India. A remote sensing based estimate. *Sustainable Cities and Society, 32*, 100–114. https://doi.org/10.1016/j.scs.2017.02.018

Skelhorn, C., Lindley, S., & Levermore, G. (2014). The impact of vegetation types on air and surface temperatures in a temperate city: A fine scale assessment in Manchester, UK. *Landscape and Urban Planning, 121*, 129–140. https://doi.org/10.1016/j.landurbplan.2013.09.012

Sobrino, J. A., Li, Z. L., Stoll, M. P., & Becker, F. (1996). Multi-channel and multi-angle algorithms for estimating sea and land surface temperature with atsr data. *International Journal of Remote Sensing, 17*(11), 2089–2114. https://doi.org/10.1080/01431169608948760

Sobrino, J. A., & Raissouni, N. (2000). Toward remote sensing methods for land cover dynamic monitoring: Application to Morocco. *International Journal of Remote Sensing, 21*(2), 353–366. https://doi.org/10.1080/014311600210876

Sobrino, José A., Jiménez-Muñoz, J. C., & Paolini, L. (2004). Land surface temperature retrieval from LANDSAT TM 5. *Remote Sensing of Environment, 90*(4), 434–440. https://doi.org/10.1016/J.RSE.2004.02.003

Sodoudi, S., Zhang, H., Chi, X., Müller, F., & Li, H. (2018). The influence of spatial configuration of green areas on microclimate and thermal comfort. *Urban Forestry and Urban Greening, 34*, 85–96. https://doi.org/10.1016/j.ufug.2018.06.002

Son, N.-T., Chen, C.-F., Chen, C.-R., Thanh, B.-X., & Vuong, T.-H. (2017). Assessment of urbanization and urban heat islands in Ho Chi Minh City, Vietnam using Landsat data. *Sustainable Cities and Society, 30*, 150–161. https://doi.org/10.1016/j.scs.2017.01.009

Steeneveld, G. J., Koopmans, S., Heusinkveld, B. G., & Theeuwes, N. E. (2014). Refreshing the role of open water surfaces on mitigating the maximum urban heat island effect. *Landscape and Urban Planning, 121*, 92–96. https://doi.org/10.1016/j.landurbplan.2013.09.001

Sun, R., Chen, A., Chen, L., & Lü, Y. (2012). Cooling effects of wetlands in an urban region: The case of Beijing. *Ecological Indicators, 20*(September), 57–64. https://doi.org/10.1016/j.ecolind.2012.02.006

Sundquist, K., Frank, G., & Sundquist, J. (2004). Urbanisation and incidence of psychosis and depression: Follow-up study of 4.4 million women and men in Sweden. *British Journal of Psychiatry, 184*(APR), 293–298. https://doi.org/10.1192/bjp.184.4.293

Tan, J., Zheng, Y., Tang, X., Guo, C., Li, L., Song, G., Zhen, X., Yuan, D., Kalkstein, A. J., Li, F., & Chen, H. (2010). The urban heat island and its impact on heat waves and human health in Shanghai. *International Journal of Biometeorology, 54*(1), 75–84. https://doi.org/10.1007/s00484-009-0256-x

The North West Green Infrastructure Think Tank. (2008). *North West Green Infrastructure Guide*. https://www.yumpu.com/en/document/read/46437820/north-west-green-infrastructure-guide.

Tran, H., Uchihama, D., Ochi, S., & Yasuoka, Y. (2006). Assessment with satellite data of the urban heat island effects in Asian mega cities. *International Journal of Applied Earth Observation and Geoinformation, 8*(1), 34–48. https://doi.org/10.1016/J.JAG.2005.05.003

Walawender, J. P., Szymanowski, M., Hajto, M. J., & Bokwa, A. (2014). Land surface temperature patterns in the urban agglomeration of Krakow (Poland) Derived from Landsat-7/ETM+ Data. *Pure and Applied Geophysics, 171*(6), 913–940. https://doi.org/10.1007/s00024-013-0685-7

Wan, Z. (1996). A generalized split-window algorithm for retrieving land-surface temperature from space. *IEEE Transactions on Geoscience and Remote Sensing, 34*(4), 892–905. https://doi.org/10.1109/36.508406

Wang, R., Gao, W., Zhou, N., Kammen, D. M., & Peng, W. (2021). Urban structure and its implication of heat stress by using remote sensing and simulation tool. *Sustainable Cities and Society, 65*. https://doi.org/10.1016/j.scs.2020.102632

Wang, T., Tu, H., Min, B., Li, Z. Z., Li, X. F., & You, Q. X. (2022). The mitigation effect of park landscape on thermal environment in shanghai city based on remote sensing retrieval method. *International Journal of Environmental Research and Public Health, 19*(5). https://doi.org/10.3390/ijerph19052949

Wang, Y., & Akbari, H. (2016a). Analysis of urban heat island phenomenon and mitigation solutions evaluation for Montreal. *Sustainable Cities and Society, 26*, 438–446. https://doi.org/10.1016/j.scs.2016.04.015

Wang, Y., & Akbari, H. (2016b). The effects of street tree planting on Urban Heat Island mitigation in Montreal. *Sustainable Cities and Society, 27*, 122–128. https://doi.org/10.1016/J.SCS.2016.04.013

Weng, Q., Lu, D., & Schubring, J. (2004). Estimation of land surface temperature-vegetation abundance relationship for urban heat island studies. *Remote Sensing of Environment, 89*(4), 467–483. https://doi.org/10.1016/j.rse.2003.11.005

Weng, Q., Rajasekar, U., & Hu, X. (2011). Modeling urban heat islands and their relationship with impervious surface and vegetation abundance by using ASTER images. *IEEE Transactions on Geoscience and Remote Sensing, 49*(10), 4080–4089. https://doi.org/10.1109/TGRS.2011.2128874

Xing, et al. (2024a). Developing a biophilic behavioural change design framework-A scoping study Urban. *Forestry & Urban Greening, 94*, 128278.

Xing, et al. (2024b). Developing an AI-based digital biophilic art curation to enhance mental health in intelligent buildings. *Sustainability, 16*(22), 9790.

Xing, et al. (2025). Exploring biophilic building designs to promote wellbeing and stimulate inspiration. *PloS one, 20*(3), Article e031737.

Yang, C., Yan, F., Lei, X., Ding, X., Zheng, Y., Liu, L., & Zhang, S. (2020). Investigating seasonal effects of dominant driving factors on urban land surface temperature in a snow-climate city in China. *Remote Sensing, 12*(18), 3006. https://doi.org/10.3390/rs12183006

Yang, J. X., Menenti, M., Wu, Z. F., Wong, M. S., Abbas, S., Xu, Y., & Shi, Q. (2021). Assessing the impact of urban geometry on surface urban heat island using complete and nadir temperatures. *International Journal of Climatology, 41*, E3219–E3238. https://doi.org/10.1002/joc.6919

Yu, X., Guo, X., & Wu, Z. (2014). Land Surface Temperature Retrieval from Landsat 8 TIRS—Comparison between Radiative Transfer Equation-Based Method, Split Window Algorithm and Single Channel Method. *Remote Sensing, 6*(12), 9829–9852. https://doi.org/10.3390/rs6109829

Zandi, R., Zanganeh, Y., Karami, M., & Khosravian, M. (2022). Analysis of the Spatio-temporal variations of thermal patterns of Shiraz city by satellite images and GIS processing. *Egyptian Journal of Remote Sensing and Space Sciences, 25*(4), 1069–1088. https://doi.org/10.1016/j.ejrs.2022.11.005

Zhou, W., Huang, G., & Cadenasso, M. L. (2011). Does spatial configuration matter? Understanding the effects of land cover pattern on land surface temperature in urban landscapes. *Landscape and Urban Planning, 102*(1), 54–63. https://doi.org/10.1016/J.LANDURBPLAN.2011.03.009

Zhang, Anqi, & Xia, Chang (2024). Scale effect on the relationship between urban landscape patterns and land surface temperature. *Sustainable Cities and Society, 117*, 2024.